IEEE Access
Multidisciplinary | Rapid Review | Open Access Journal

Received March 10, 2021, accepted March 26, 2021, date of publication March 30, 2021, date of current version April 8, 2021.

Digital Object Identifier 10.1109/ACCESS.2021.3069851

Study on the Harmonic Loss of Permanent Magnet Toroidal Space Motor for Hybrid Electric Vehicles

XIN LIU[1,2], HAO FENG[1], AND XIAOYUAN WANG[2]
[1]Tianjin Key Laboratory of Modern Electromechanical Equipment Technology, Tiangong University, Tianjin 300387, China
[2]School of Electrical and Information Engineering, Tianjin University, Tianjin 300072, China

Corresponding author: Xin Liu (liuxin@tiangong.edu.cn)

This work was supported in part by the National Natural Science Foundation of China (NSFC) under Grant 51875408, and in part by the State Foundation for Studying Abroad of China Scholarship Council.

ABSTRACT Based on magnetic gear transmission principle, permanent magnet toroidal space motor for hybrid electric vehicles with dual-rotor drive is proposed in this paper, harmonic loss caused by toroidal space relative motion of two rotors is conducted in hybrid drive mode. According to the structural principle of toroidal space motor, the speed of permanent magnet teeth of planet and worm inner rotor are decomposed to the revolution and rotation planes respectively. On the two planes, the frequency of alternating magnetic field at toroidal stator, planet and worm inner rotor are derived. At iron core and permanent magnetic teeth of stator and rotor, the magnetic field of revolution and rotation components are simulated. Combining with the speed relationship of toroidal space motor, the harmonic losses of revolution component and rotation component are analyzed in hybrid drive mode. The influence of speed matching of two rotors and toroidal stator material on harmonic loss are discussed. The results indicate that harmonic loss of permanent magnet toroidal space motor for hybrid electric vehicles can be reduced effectively by reducing relative speed of two rotors and adopting amorphous alloy for toroidal stator.

INDEX TERMS Toroidal space motor, dual-rotor drive, harmonic loss, speed matching.

I. INTRODUCTION

Due to the high efficiency and low emission characteristics, hybrid electric vehicles have attracted more and more attention in recent decades [1]–[4], and its hybrid power integrated system is one of the key components. Currently, the hybrid power integrated system can be divided into mechanical type and electromagnetic type [5]. Mechanical hybrid power integrated system is usually composed of motor, generator, engine and several sets of planet mechanism. By controlling the working state of each part, hybrid electric vehicles can operate in multiple operation modes [6]–[10]. However, the mechanical hybrid system is equipped with two motors and one engine, thus its overall structure size of the system is relatively large. Because mechanical planet mechanism is adopted for power transmission in mechanical hybrid system [11], the problems of noise, vibration and inconvenient maintenance are inevitable. In recent years, in order to solve these problems existed in the mechanical hybrid power integrated system, electromagnetic power integrated system has developed rapidly. This kind of system adopts the dual-rotor motor instead of the mechanical planet in mechanical hybrid system [12]–[18]. By controlling the dual-rotor motor, functions of mechanical planet can be realized in the electromagnetic hybrid system [19]. However, the shafts of this kind of dual-rotor motors are parallel, and the electrical components are arranged densely, which leads the heat dissipation performance of the motor is not good.

In this paper, a novel permanent magnet toroidal hybrid power system is proposed. This electromagnetic power integrated system is mainly composed of permanent magnet toroidal space motor and engine, it can realize multiple working modes to ensure efficient operation of the engine. The structure diagram is shown in Fig. 1. ICE is the abbreviation of internal combustion engine, and BAT is the abbreviation of battery. Permanent magnet toroidal space motor is the core component of the hybrid power system. The motor has two mechanical ports that connect with engine and axle of

The associate editor coordinating the review of this manuscript and approving it for publication was Wei Xu.

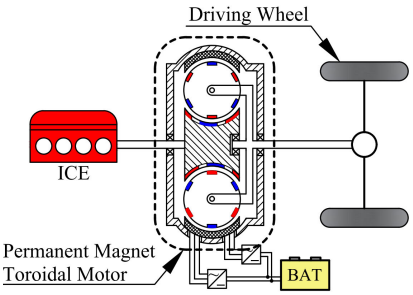

FIGURE 1. Permanent magnet toroidal hybrid power system.

driving wheel respectively, and an electrical port connected with three-phase winding. Power integration and power distribution are realized through the mechanical and electrical ports. The permanent magnet toroidal space motor for hybrid electric vehicles can realize the integration of motor, generator and reducer, so the overall structure is more compact than mechanical hybrid system.

In terms of power transmission, the toroidal motor adopts magnetic gear meshing transmission [20], which avoids the problems of mechanical transmission effectively. Compared with other dual-rotor motors, the shaft of planet is perpendicular to the output shaft of planet carrier rotor in space [21], thus heat dissipation performance of toroidal motor is improved. Meanwhile, the winding of toroidal stator and permanent magnet teeth of worm inner stator are spiral structure, which make the permanent magnet teeth of planet mesh with multiple windings and permanent magnet teeth at the same time. So toroidal space motor can increase the number of meshing magnet teeth greatly. The magnetic teeth meshing area of traditional dual-rotor motor and toroidal dual-rotor space motor is shown in Fig. 2.

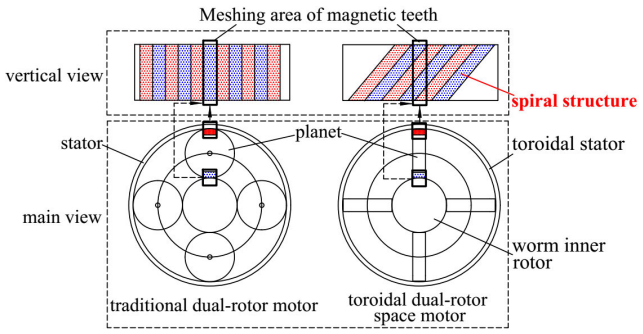

FIGURE 2. Comparison of magnetic teeth meshing area.

Due to kinematic characteristics of the permanent magnet toroidal hybrid power system, when the toroidal driving system is working except hybrid mode, the speed of worm inner rotor is zero. The meshing relationship of permanent magnet teeth between planets and worm inner rotor makes that there is no relative movement between the permanent magnetic teeth. But when the permanent magnet toroidal hybrid power system operates in hybrid mode, the input speed of worm inner rotor is less than the output speed of planet carrier rotor, which causes relative motion between the permanent magnet teeth of worm inner rotor and planets. The relative motion of the permanent magnet teeth can generate an alternating magnetic field, which will causes harmonic loss in toroidal motor. Different input speed combinations of the two input ports can achieve the same output speed of planet carrier rotor. And when the output speed of planet carrier rotor is constant, the harmonic loss caused by different speed combinations of the two rotors is different. Therefore, it is necessary to analyze the harmonic loss of toroidal motor in hybrid mode. Under the premise of constant output speed, the harmonic loss caused by the relative motion of permanent magnet teeth can be reduced by matching the speed of two rotors. The harmonic loss of toroidal stator is the biggest. The material of toroidal stator has influence on the loss of toroidal stator. In order to reduce harmonic loss of the motor further, harmonic loss of toroidal stator can be reduced by choosing reasonable material of toroidal stator.

In this paper, based on the working principle of the permanent magnet toroidal space motor for HEV, the speed of permanent magnet teeth on planet and worm inner rotor are analyzed on the plane of revolution and rotation. The frequency of alternating magnetic field is deduced at the main parts of toroidal motor. The magnetic field of radial section and axial section of the motor are simulated by finite element method. The influences of different speed matching and different materials of toroidal stator on the harmonic loss are compared.

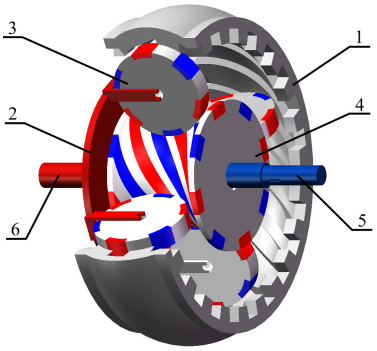

FIGURE 3. Structure diagram of permanent magnet toroidal space motor for hybrid electric vehicles.

II. PRINCIPLE OF HYBRID DRIVE

A. PRINCIPLE OF STRUCTURE

The structure diagram of permanent magnet toroidal space motor for hybrid electric vehicles is shown in Fig. 3. The toroidal motor is mainly composed of toroidal stator 1, planet carrier rotor 2, planet 3, worm inner rotor 4, input shaft of worm inner rotor 5 and output shaft of planet carrier rotor 6. The three-phase winding is embedded spirally in toroidal stator. The permanent magnet teeth with radial magnetization are attached on the circumference of planets. The helical permanent magnet teeth are attached on the surface of worm

inner rotor. The shaft of planet is perpendicular to the output shaft of worm inner rotor.

In the hybrid mode, the toroidal stator winding is supplied with three-phase alternating current, and a spiral rotating magnetic field is generated. The worm inner rotor is connected to the engine. The permanent magnet teeth of planet are subjected to two forces, the electromagnetic force of spiral rotating magnetic field and the magnetic force of permanent magnetic teeth of worm inner rotor. Under the action of electromagnetic force and magnetic force, the permanent magnet teeth of planet are driven to rotate along toroidal spirally. Thus, the planets rotate on their axes while they revolve around the shaft of planet carrier rotor. The revolution component of planet drives planet carrier rotor to rotate. The power output of permanent magnet toroidal space motor is realized.

B. SPEED ANALYSIS

The revolution and rotation planes of planets intersect perpendicularly, which makes the motion trajectory of permanent magnet teeth of planet have three-dimensional spatiality. Take a permanent magnet tooth of the planet for analysis, the trajectory of the permanent magnet tooth on planet is circular spiral as shown in Fig. 4.

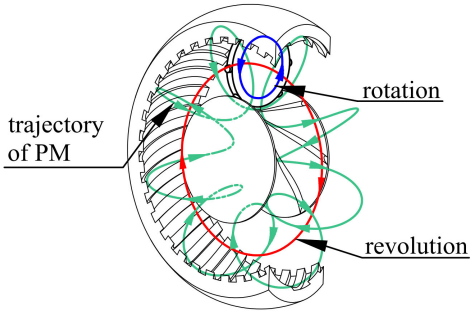

FIGURE 4. Trajectory of the permanent magnetic tooth on planet.

For the convenience of analysis, the speed of permanent magnet tooth on planet is decomposed to the revolution plane and rotation plane respectively. On revolution plane, the speed of the permanent magnet tooth of planet is equal to the speed n_2 of planet carrier rotor. According to the principle of permanent magnet toroidal transmission, the output speed of planet carrier rotor in hybrid mode can be obtained as

$$n_2 = \frac{1}{p_1 - p_4}(p_1 n_1 - p_4 n_4) \tag{1}$$

where $p_1$is the pole-pair number of toroidal stator rotating magnetic field, $p_4$is the permanent magnet tooth pair number of worm inner rotor, $n_1$is the speed of rotating magnetic field, n_4 is the speed of worm inner rotor.

On rotation plane, the speed of permanent magnet tooth on planet is equal to the rotation speed n_3 of planet. According to the transmission relationship between planet and worm inner rotor, the rotation speed of planet can be deduced as

$$n_3 = \left(1 + \frac{p_4}{p_3}\right) n_2 - \frac{p_4}{p_3} n_4 \tag{2}$$

where $p_3$is the permanent magnetic tooth pair number of planets.

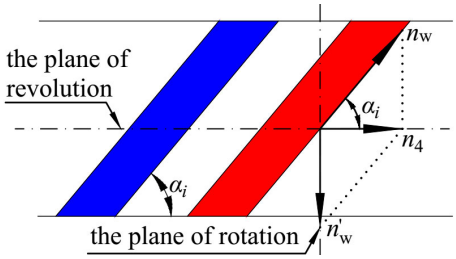

FIGURE 5. Speed decomposition of PM tooth on worm inner rotor.

In the same manner, the speed of permanent magnet tooth on worm inner rotor can be decomposed to the two planes. The spiral angle of permanent magnet teeth on worm inner rotor is α_i. The expanded view for speed decomposition of permanent magnet tooth on worm inner rotor is shown as Fig. 5. n_w is the speed of convected motion, which is related to the spiral angle α_i of permanent magnet tooth on worm inner rotor, and n'_w is the rotation speed of permanent magnet tooth on worm inner rotor.

Obviously, the revolution speed of permanent magnet tooth of worm inner rotor is equal to the speed n_4. Based on the spiral angle α_i of permanent magnet tooth, the rotation speed n'_w of permanent magnet tooth on worm inner rotor can be expressed as

$$n'_w = n_4 \tan \alpha_i \tag{3}$$

III. FREQUENCY AND AMPLITUDE ANALYSIS OF ALTERNATING MAGNETIC FIELD

Based on the above speed analysis, it can be known that the permanent magnet teeth of dual-rotor have relative motion in both revolution and rotation planes. The relative motion of permanent magnet teeth generates an alternating magnetic field, which produces harmonic loss in permanent magnet toroidal space motor for HEV.

The radial section of permanent magnet toroidal space motor for HEV is taken to analyze the harmonic loss caused by relative revolution motion. Without considering rotation of planets, the equivalent model of permanent magnet toroidal space motor for HEV is shown in Fig. 6(a). The four planets of toroidal motor are equivalent to an intermediate rotor with permanent magnet teeth. The worm inner rotor is an inner rotor with permanent magnet teeth, and the toroidal stator is an outer stator. The axial section of toroidal motor passing through planet is taken to analyze the harmonic loss caused by relative rotation motion. Without considering revolution of planets, the equivalent model of permanent magnet toroidal space motor for HEV is shown in Fig. 6(b).

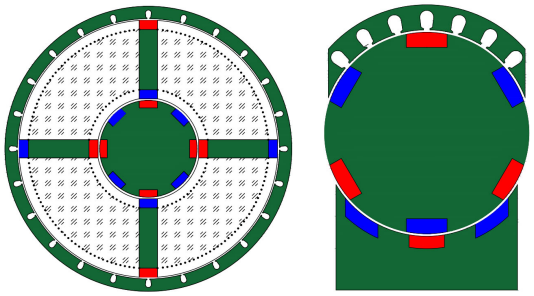

FIGURE 6. Equivalent model of permanent magnet toroidal space motor for HEV. (a) radial section, (b) axial section.

The harmonic loss generated by the two kinds of motion components includes iron core loss and eddy current loss. The iron core loss exists in iron core of toroidal stator, planets and worm inner rotor. The eddy current loss exists in permanent magnet teeth of planets and worm inner rotor.

The iron core loss P_{Fe} caused by harmonic at each part of toroidal space motor can be obtained by Bertotti model

$$P_{\mathrm{Fe}} = P_{\mathrm{h}} + P_{\mathrm{e}} + P_{\mathrm{a}} = K_h f B^{\alpha} + K_e f^2 B^2 + K_a f^{1.5} B^{1.5} \quad (4)$$

where, P_{h}, P_{e} and $P_{\mathrm{a}}$are hysteretic loss, eddy current loss and additional loss of toroidal space motor respectively; f is the frequency of alternating magnetic field; B is the flux density of alternating magnetic field; α is coefficient of hysteretic loss; K_h, K_e and K_a are loss factors related to material properties.

In order to analyze eddy current loss in the revolution plane and rotation plane respectively, the displacement current is ignored, and the eddy current density of revolution plane and rotation plane can be expressed as

$$\nabla \times \left(\frac{1}{\mu} (\nabla \times A_z - B_r) \right) + \sigma \frac{\partial A_z}{\partial t} = J_{\mathrm{sz}} \quad (5)$$

where B_r is remanence density of permanent magnet tooth; $\sigma$is electric conductivity of permanent magnet tooth; μ is magnetic permeability of material, it changes with the magnetic flux density and affects the distribution of eddy current for nonlinear materials; A_z is magnetic vector potential; t is time; $J_{\mathrm{sz}}$is the current density of axial eddy current of toroidal space motor when the eddy current loss of revolution component is analyzed, $J_{\mathrm{sz}}$is the current density of axial eddy current of planet when the eddy current loss of rotation component is analyzed.

The eddy current loss P_{PM} caused by harmonic at each permanent magnet tooth can be calculated by the eddy current loss formula as follow

$$P_{\mathrm{PM}} = \int_V \frac{|J_{\mathrm{sz}}|^2}{\sigma} \mathrm{d}V = L \int \int_s \frac{|J_{\mathrm{sz}}|^2}{\sigma} \mathrm{d}S \quad (6)$$

where S is section area of eddy current; L is axial length of permanent magnet toroidal space motor when the eddy current loss of revolution component is analyzed; L is the thickness of planet when the eddy current loss of rotation component is analyzed.

It can be seen from (4) and (6), the harmonic loss of permanent magnet toroidal space motor is related to the frequency of magnetic density fluctuation and amplitude of magnetic flux density.

A. FREQUENCY ANALYSIS

The harmonic magnetic fields at the toroidal stator, planet and worm inner rotor are different, which make the frequencies of magnetic flux density in these three parts are different. They are related to the speed and magnetic teeth number of each part.

On revolution plane, the magnetic density of toroidal stator changes with the combined action of revolution components of permanent magnetic teeth on planets and worm inner rotor. The frequency of magnetic density fluctuation at yoke and tooth of toroidal stator can be expressed as

$$f_{\mathrm{s}} = \frac{|n_2 z_v - 2 n_4 p_4|}{120} \quad (7)$$

where $z_v$is the number of planets.

The magnetic density at planet and worm inner rotor changes with the relative revolution motion components between permanent magnet teeth of planet and worm inner rotor. The frequency of magnetic density fluctuation of planet on revolution plane is

$$f_{\mathrm{p}} = \frac{|n_2 - n_4|\, z_v}{120} \quad (8)$$

The frequency of magnetic density fluctuation of worm inner rotor on revolution plane can be obtained as

$$f_{\mathrm{w}} = \frac{|n_2 - n_4|\, p_4}{60} \quad (9)$$

On rotation plane, the frequency of magnetic density fluctuation of toroidal motor can be obtained in the same manner. The magnetic density of toroidal stator on rotation plane changes with the combined action of rotation components of permanent magnetic teeth. The frequency of magnetic density fluctuation at yoke and tooth of toroidal stator can be expressed as

$$f'_{\mathrm{s}} = \frac{|n_3 p_3 - n'_w p'_4|}{60} \quad (10)$$

where p'_4 is the number of permanent magnet tooth pair of worm inner rotor on axial section.

The magnetic density at planet and worm inner rotor changes with the relative rotation motion component between permanent magnet teeth of planet and worm inner rotor. The frequency of magnetic density fluctuation of planet on revolution plane can be obtained as

$$f'_{\mathrm{p}} = \frac{|n_3 - n'_w|\, p_3}{60} \quad (11)$$

The frequency of magnetic density fluctuation of worm inner rotor on rotation plane can be expressed as

$$f'_w = \frac{|n_3 - n'_w| p'_4}{60} \tag{12}$$

B. MAGNETIC FLUX DENSITY ANALYSIS

In order to analyze the magnetic flux density at main parts, the magnetic field of equivalent toroidal motor on radial and axial sections are simulated. On the two sections of permanent magnet toroidal space motor for HEV, the observation points are selected to analyze magnetic field. The positions of observation points are shown in Fig. 7.

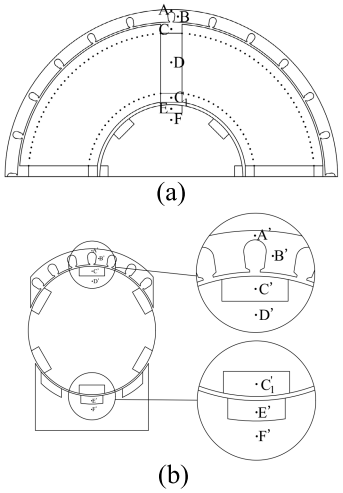

FIGURE 7. Positions of observation points. (a) points on radial section, (b) points on axial section.

The structure parameters of permanent magnet toroidal space motor for simulation are presented in Table 1. The input speed of worm inner rotor is set to 2000r/min, the output speed of planet carrier rotor is set to 2500r/min, and the simulation time is $t = 120$ms.

Fig. 8 shows the tangential and radial flux density of toroidal motor with respect to time, that caused by revolution component.

1) From the number of magnetic flux density fluctuation of toroidal stator iron core, it can be known that the period of magnetic flux density fluctuation is 20ms with frequency 50Hz. The simulation result is consistent with theoretical derivation. The magnetic flux density amplitude of tangential is greater than that of radial at toroidal stator yoke, which is the main part of the tooth. This is because the magnetic induction lines at stator yoke are distributed along circumference, and most of the magnetic induction lines at tooth are distributed along radial direction. Based on above analysis, it can be concluded that the iron core loss of toroidal stator is mainly caused by two parts, that is the tangential magnetic density at yoke and radial magnetic density at tooth.

TABLE 1. Parameters of the motor structure.

Parameters	Value
Slot number of toroidal stators	24
Pole-pair number of toroidal stators	2
Number of planets	4
Number of PM teeth of planet	6
Number of PM teeth of worm inner rotor	8
Outer diameter of waist of the toroidal stator	232mm
Inner diameter of waist of the toroidal stator	204mm
Diameter of planet	80mm
Thickness of planet	10mm
Diameter of waist of the worm inner rotor	76mm
Length of the radial of the motor	80mm
Thickness of PM teeth	5mm
Air gap	1mm

2) The magnetic flux density at planet changes periodically. The frequency of magnetic density fluctuation is 16.6Hz, which is basically consistent with theoretical derivation. The slots of permanent magnet on planet can cause more harmonic, thus there are many small ripples on the magnetic flux density curve of planet. At permanent magnet tooth of planet, the magnetic flux density amplitude of radial is greater than that of tangential. It is due to that the permanent magnetic teeth of planet are magnetized radially. At the iron core of planet, the average values of tangential and radial magnetic flux density are the same approximately, and they are relatively small.

3) There are many small ripples on magnetic flux density curve of worm inner rotor, which is due to the slots of permanent magnet arranged on worm inner rotor. From the number of magnetic flux density fluctuations, it can be known that the frequency of magnetic density fluctuation is 33.3Hz, which is also consistent with theoretical derivation. The magnetic flux density amplitude of radial is greater than that of tangential at permanent magnet tooth of worm inner rotor, which is because of the permanent magnetic tooth of planet is magnetized radially. At the iron core of worm inner rotor, the tangential magnetic flux density value fluctuates around 0 with an average value 0.15T. The amplitude of radial magnetic flux density fluctuation is relatively large, and its average value is 0.45T.

Affected by revolution motion component, the amplitude and frequency of magnetic flux density at main parts of permanent magnet toroidal space motor for HEV are shown in Table 2.

Fig. 9 shows the tangential and radial flux density at main parts with respect to time, that caused by rotation motion component.

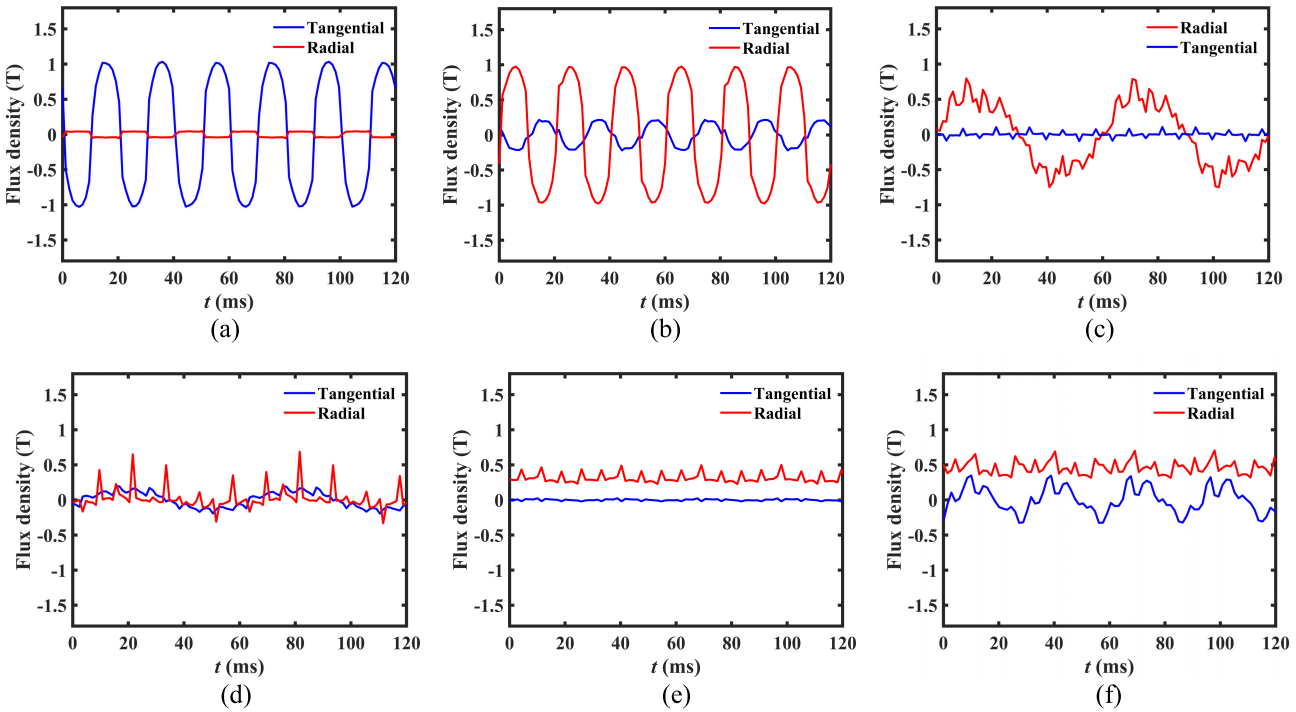

FIGURE 8. Magnetic flux density caused by revolution component. (a) yoke of toroidal stator iron core. (b) tooth of toroidal stator iron core, (c) PM tooth of planet, (d) iron core of planet, (e) PM tooth of worm inner rotor, (f) iron core of worm inner rotor.

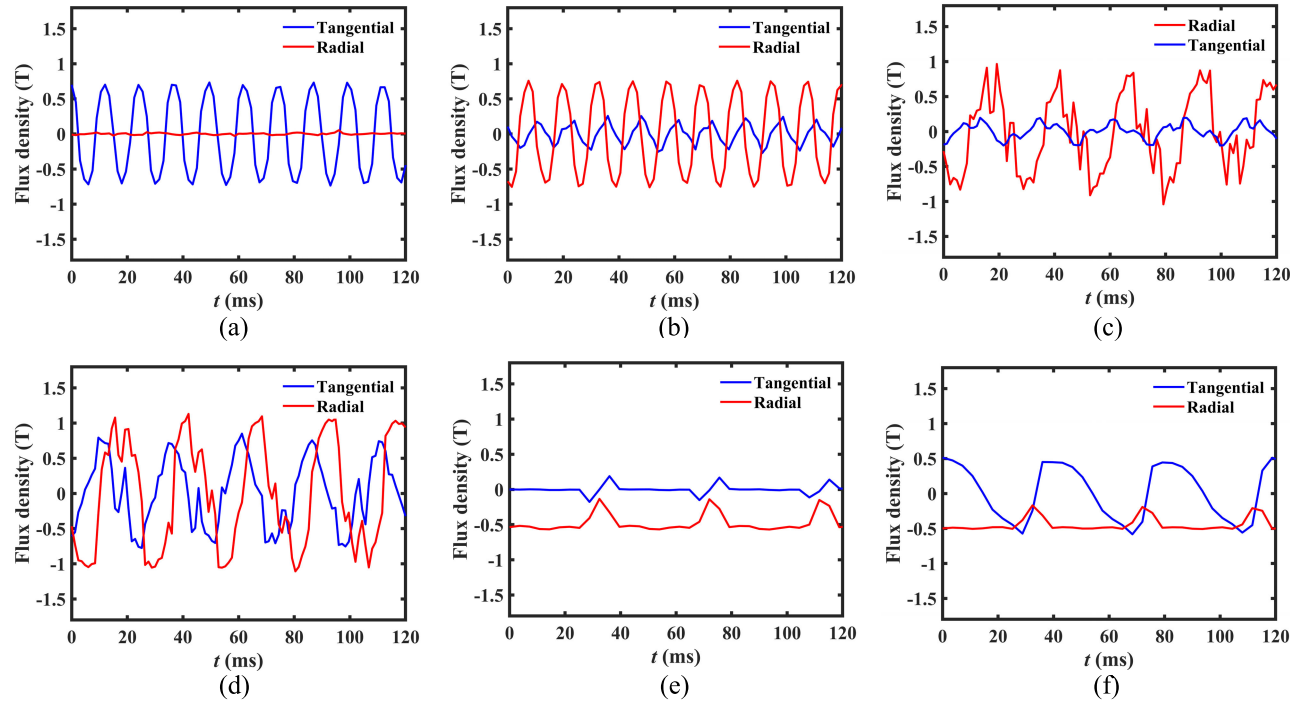

FIGURE 9. Magnetic flux density caused by rotation component. (a) yoke of toroidal stator iron core. (b) tooth of toroidal stator iron core, (c) PM tooth of planet, (d) iron core of planet, (e) PM tooth of worm inner rotor, (f) iron core of worm inner rotor.

1) The amplitude of magnetic flux density at permanent magnet tooth and iron core of planet is relatively larger, and that at permanent magnet tooth and iron core of worm inner rotor is smaller. Because the magnetic induction line is distributed along the axial direction at yoke of toroidal stator, the tangential magnetic flux density at yoke is the main

TABLE 2. Magnetic density change with revolution motion component.

Position	B_{max}	f
Core of toroidal stator	1.1T	50Hz
PM tooth of planet	0.8T	16.7Hz
Core of planet	0.7T	16.7Hz
PM tooth of worm inner rotor	0.45T	33.3Hz
Core of worm inner rotor	0.6T	33.3Hz

part. The magnetic induction line of tooth is mainly along the radial direction, thus the magnetic flux density amplitude of radial is greater than that of tangential at tooth of toroidal stator. The permanent magnet teeth of planet and worm inner rotor are magnetized radially, thus the magnetic flux density amplitude of radial is larger than that of tangential. At iron core of planet, the magnetic flux density amplitude of radial is close to that of tangential, and amplitudes of them both are very large, which indicate that they will cause large loss in iron core of planet. At iron core of worm inner rotor, the magnetic flux density amplitudes of radial and tangential are the same, but the magnetic flux density average value of radial is larger than that of tangential. It shows that iron core loss of worm inner rotor is mainly caused by tangential magnetic flux density.

2) From the number of magnetic flux density fluctuation, it can be known that the periods of magnetic flux density fluctuation at iron core of toroidal stator, planet and worm inner rotor are 11.6ms, 26ms and 42.3ms respectively. The corresponding frequency of magnetic flux density fluctuation are 86.2Hz, 39.1Hz and 23.6Hz respectively, that are consistent with the theoretical results. Under the influence of permanent magnetic slots on planet and worm inner rotor, there are small ripples in magnetic flux density curve.

Influenced by rotation motion component, the amplitude and frequency of magnetic flux density at main parts of permanent magnet toroidal space motor for HEV are shown in Table 3.

TABLE 3. Magnetic density change with rotation motion component.

Position	B_{max}	f
Iron core of toroidal stator	0.9T	86.2Hz
PM tooth of planet	1.0T	39.1Hz
Iron core of planet	1.1T	39.1Hz
PM tooth of worm inner rotor	0.6T	23.6Hz
Iron core of worm inner rotor	0.5T	23.6Hz

IV. LOSS ANALYSIS AND OPTIMIZATION

A. LOSS ANALYSIS

In order to obtain the harmonic losses at main parts, the radial and axial sections of permanent magnet toroidal space motor for HEV are simulated, and the harmonic losses of main parts are shown in Table 4. It can be known that the total harmonic loss caused by rotation motion component is greater than that caused by revolution motion component. The reason is that rotation speed of planet is greater than revolution speed of planet. In the same period, the meshing area of magnetic teeth in rotation plane is larger than that in revolution plane. In both cases, iron core loss of toroidal stator is the largest. At iron core of planet and permanent magnet teeth of worm inner rotor, the harmonic loss caused by rotation component is higher than that caused by revolution component. At iron core of worm inner rotor, the harmonic loss of rotation component is lower than that caused by revolution component. This is because the amplitude and fluctuation frequency of magnetic flux density at iron core of worm inner rotor caused by revolution component are all greater than that caused by rotation component.

TABLE 4. Harmonic loss of each part.

Position	Revolution	Rotation
Iron core of toroidal stator	78W	81W
PM tooth of planet	18W	24W
Iron core of planet	22W	60W
PM tooth of worm inner rotor	18W	51W
Iron core of worm inner rotor	30W	12W
Total harmonic loss	166W	228W

In order to reduce harmonic loss in permanent magnet toroidal space motor for HEV, relative motion of the dual-rotor can be changed by speed matching, and frequency of magnetic flux density fluctuation at main parts can be reduced.

B. INFLUENCE OF INPUT SPEED ON HARMONIC LOSS

Based on the output speed characteristic of permanent magnet toroidal space motor for HEV, it can be known that there are different input speed matching of rotating magnetic field and worm inner rotor to keep the output speed of planet carrier rotor constant. Different speed matching makes the frequency of magnetic flux density fluctuation of each part different. Under the output speed of planet carrier rotor remains unchanged, the speed of rotating magnetic field and inner worm rotor are one-to-one correspondence. Therefore, the influence of input speed on the frequency of magnetic flux density fluctuation needs to be analyzed. Taking the input speed of worm inner rotor as an example, the relationships between frequency of flux density fluctuation and input speed of worm inner rotor are shown in Fig. 10.

Speed range A is the effective range of speed n_4, and it changes with the output speed n_2 of planet carrier rotor. Under the speed $n_2 = 2500$r/min, the speed n_4 of worm inner rotor is

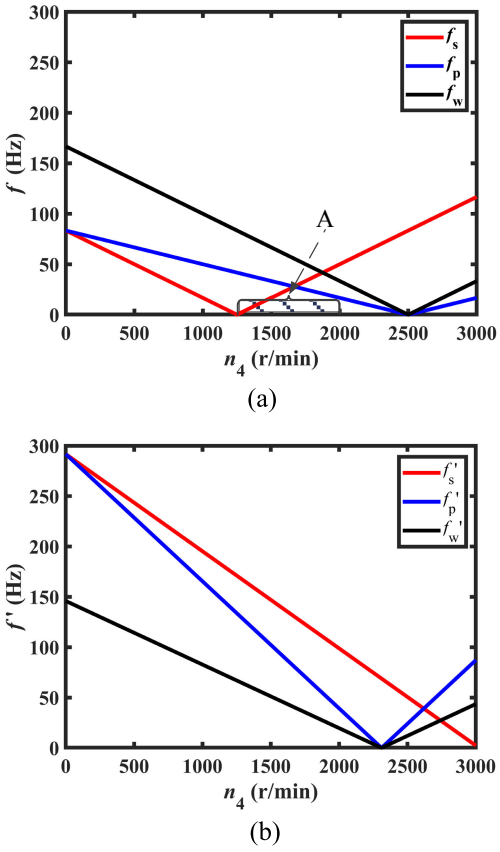

FIGURE 10. Relationship between frequency and input speed n_4 of worm inner rotor. (a) revolution frequency component, (b) rotation frequency component.

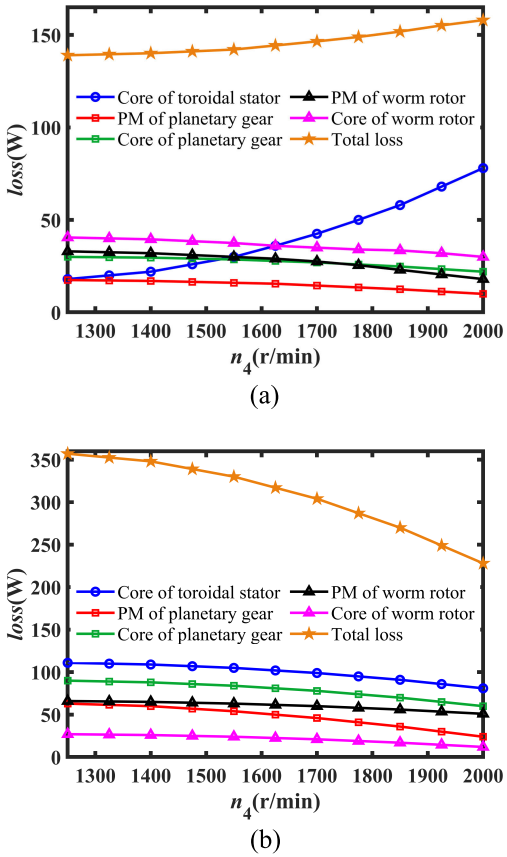

FIGURE 11. Changes of harmonic loss with n_4. (a) revolution component, (b) rotation component.

1250r/min with the minimum speed n_1 of rotating magnetic field. When the speed n_1 of rotating magnetic field reaches the maximum speed 1500r/min, the speed n_4 of worm inner rotor is 2000r/min. Thus, the effective range A of speed n_4 is 1250-2000r/min when output speed n_2 remains 2500r/min. The changes of harmonic loss with input speed n_4 of worm inner rotor are shown in Fig. 11.

It can be known that under the output speed of planet carrier rotor remains unchanged:

1) For the harmonic loss caused by revolution motion component, the iron core loss of toroidal stator caused by revolution component increases significantly with the speed of worm inner rotor increase, and losses of planet and worm inner rotor decrease. The harmonic loss is correlated with frequency of alternating magnetic field positively. From frequency of toroidal stator, it can be obtained that the greater speed of worm inner rotor, the greater frequency of magnetic density fluctuation of toroidal stator, thus iron core loss of toroidal stator can increase. From frequency of planet and worm inner rotor, it can be known that the greater speed of worm inner rotor, the smaller frequency of magnetic density fluctuation of planet and worm inner rotor, so harmonic loss of planet and worm inner rotor can reduce.

2) For the harmonic loss caused by rotation motion component, the harmonic losses of toroidal stator, planet and worm inner rotor all decrease with the speed of worm inner rotor increase. The speed of planet decreases with the speed of worm inner rotor increase. Because the speed of planet is the largest in axial section of the motor, the relative speed of permanent magnet teeth on axial section decreases with the speed of planet decrease. The frequency of magnetic flux density fluctuation of each part decrease, thus total harmonic loss of the motor can decrease.

3) The change trend of harmonic loss is consistent with frequency of magnetic flux density. Because harmonic loss is positively correlated to frequency and amplitude of magnetic flux density. The frequency will changes with n_4, but amplitude of magnetic flux density will not change, thus the harmonic loss is positively correlated to the frequency of magnetic flux density. The relationship between frequency and speed n_4 has verified the accuracy of harmonic loss curve.

By increasing the speed of worm inner rotor, the harmonic loss caused by rotation component can be reduced under the output speed of planet carrier rotor is constant, but the harmonic loss caused by revolution component will increase. The increase of the harmonic loss caused by revolution

component is small about 13.6%, and the decrease of the harmonic loss caused by rotation component is about 36.1%. With comprehensive consideration, the relative speed of two rotors can be reduced by increasing the speed of worm inner rotor under the output speed of planet carrier rotor remains unchanged, and total harmonic loss of the motor will decrease.

C. INFLUENCE OF MATERIAL ON HARMONIC LOSS

Under the influence of revolution component, the harmonic loss of planet and worm inner rotor decrease with the speed of worm inner rotor increase, but the iron core loss of toroidal stator increases. The loss of toroidal stator accounts for a large proportion of total loss. In order to reduce proportion of iron core loss of toroidal stator, the amplitude of toroidal stator iron core loss can be reduced by changing the material of toroidal stator iron core. Silicon steel sheet (DW465-50) material is used for toroidal stator iron core in the above analysis. In the following, soft magnetic composite (SMC) and amorphous alloy are selected for analysis of harmonic loss. The radial section of the motor is simulated, harmonic losses of revolution component with different materials are shown in Fig. 12.

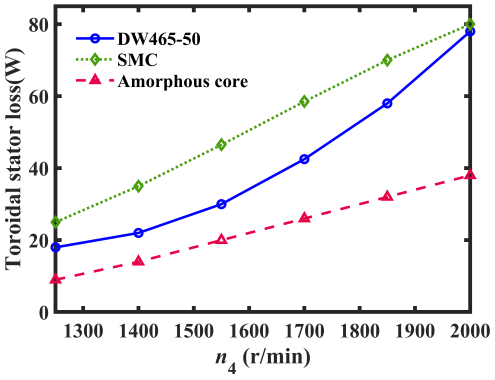

FIGURE 12. Harmonic losses of revolution component with different materials.

Under the output speed of planet carrier rotor remains unchanged, the losses caused by revolution component of toroidal stator with three materials all decrease with the speed of worm inner rotor increase. The iron core loss of toroidal stator used amorphous material is the smallest. The iron core loss of toroidal stator with SMC is greater than that with DW465-50. With the speed of worm inner rotor increase, the amplification of harmonic loss with DW465-50 increasing, while that with SMC is unchanged. The greater speed of worm inner rotor, the higher frequency of flux density fluctuation of revolution component at toroidal stator. Thus material of SMC is suitable for high-frequency applications. The frequency of magnetic field fluctuation of toroidal stator is relatively low, advantage of SMC is not significant. With comprehensive consideration, the iron core loss of toroidal

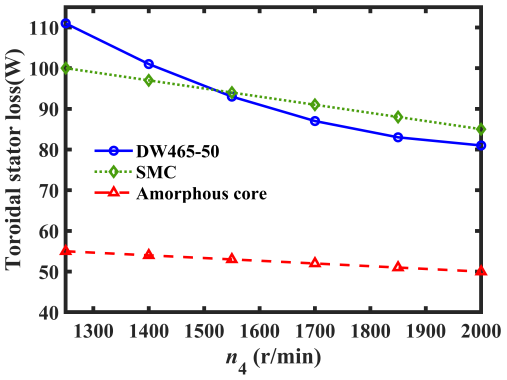

FIGURE 13. Harmonic losses of rotation component with different materials.

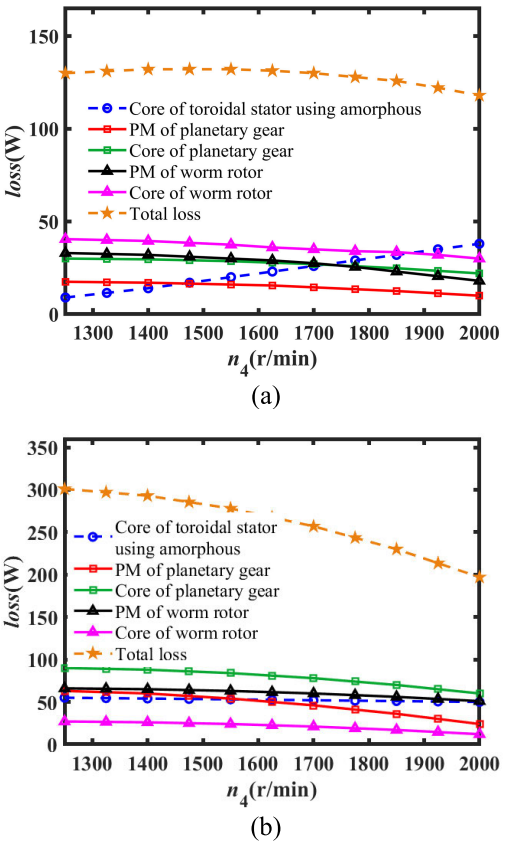

FIGURE 14. Harmonic loss of toroidal motor with amorphous alloy. (a) revolution component, (b) rotation component.

stator caused by revolution component can be reduced with the material of amorphous alloy.

The harmonic losses of rotation component with different materials are shown in Fig. 13.

It can be seen from Fig. 13 that the harmonic losses of toroidal stator with three materials all decrease with the speed of worm inner rotor increase. The iron core loss of toroidal stator with amorphous alloy is the least. The iron core loss of toroidal stator with SMC is close to that with

DW465-50. The harmonic loss toroidal stator with SMC is less than that with DW465-50 when the speed of worm inner rotor is small. With the speed of worm inner rotor increase, the harmonic loss of SMC is greater than that of DW465-50. The smaller speed of worm inner rotor, the higher frequency of flux density fluctuation of rotation component at toroidal stator. Thus the material of SMC is suitable for high-frequency applications. The frequency of magnetic flux density fluctuation of toroidal stator did not reach the optimal working frequency of SMC. With comprehensive consideration, the iron core loss of toroidal stator caused by rotation component can be reduced with the material of amorphous alloy.

Under toroidal stator with the material of amorphous alloy, harmonic losses of each part of permanent magnet toroidal space motor for HEV are shown in Fig. 14.

Under toroidal stator with the material of amorphous alloy, harmonic loss of toroidal stator caused by revolution component increases with the speed of worm inner rotor increase, the loss of toroidal stator accounts in total harmonic loss decreases, so total harmonic loss caused by revolution component is reduced. The harmonic loss of toroidal stator with the material of amorphous alloy caused by rotation component is reduced further, and total harmonic loss caused by rotation component is also reduced.

V. CONCLUSION

A permanent magnet toroidal space motor for HEVs is proposed in this paper. The harmonic losses caused by two different motion components are analyzed by finite element simulation, and influences of speed matching and material on harmonic loss are discussed. The following conclusions are obtained:

1) In the radial plane and axial plane, the harmonic losses caused by revolution component and rotation component are analyzed respectively. The total harmonic loss of each part of toroidal motor caused by rotation motion component is greater than that caused by revolution motion component, and harmonic loss of toroidal stator is the largest in two harmonic loss components.

2) Under the output speed of planet carrier rotor remains unchanged, the speed of planet carrier rotor is always greater than speed of worm inner rotor in hybrid mode. The relative speed of permanent magnet teeth of worm inner rotor and planet can be reduced effectively by increasing the speed of worm inner rotor. The total harmonic loss caused by rotation component decreases with the speed of worm inner rotor increase, and total harmonic loss caused by revolution component increased slightly.

3) The iron core loss of toroidal stator with material of amorphous alloy is smaller than that with material of silicon steel sheet. Under the output speed of planet carrier rotor remains unchanged, iron core loss of toroidal stator with amorphous alloy account for a smaller proportion of total loss, thus total harmonic loss caused by revolution component decreases with the speed of worm inner rotor increase. In addition, material of soft magnetic composite can also reduce harmonic loss of toroidal stator under the motor can achieve high-frequency operation.

REFERENCES

[1] J. Snoussi, S. B. Elghali, M. Benbouzid, and M. F. Mimouni, "Optimal sizing of energy storage systems using frequency-separation-based energy management for fuel cell hybrid electric vehicles," *IEEE Trans. Veh. Technol.*, vol. 67, no. 10, pp. 9337–9346, Oct. 2018.

[2] G. Jinquan, H. Hongwen, P. Jiankun, and Z. Nana, "A novel MPC-based adaptive energy management strategy in plug-in hybrid electric vehicles," *Energy*, vol. 175, pp. 378–392, May 2019.

[3] X. Tang, X. Hu, W. Yang, and H. Yu, "Novel torsional vibration modeling and assessment of a power-split hybrid electric vehicle equipped with a dual-mass flywheel," *IEEE Trans. Veh. Technol.*, vol. 67, no. 3, pp. 1990–2000, Mar. 2018.

[4] K. Tammi, T. Minav, and J. Kortelainen, "Thirty years of electro-hybrid powertrain simulation," *IEEE Access*, vol. 6, pp. 35250–35295, 2018.

[5] F. Cerna, M. Pourakbarl-Kasmel, M. Lehtonen, and J. Contreras, "Efficient automation of an HEV heterogeneous fleet using a two-stage methodology," *IEEE Trans. Veh. Technol.*, vol. 67, no. 12, pp. 11390–11401, Oct. 2019.

[6] A. Ghayebloo and A. Radan, "Superiority of dual-mechanical-port-machine-based structure for series–parallel hybrid electric vehicle applications," *IEEE Trans. Veh. Technol.*, vol. 65, no. 2, pp. 589–602, Feb. 2016.

[7] H. Fathabadi, "Plug-in hybrid electric vehicles: Replacing internal combustion engine with clean and renewable energy based auxiliary power sources," *IEEE Trans. Power Electron.*, vol. 33, no. 11, pp. 9611–9618, Nov. 2018.

[8] Z. Song, C. Liu, and H. Zhao, "Investigation on magnetic force of a flux-modulated double-rotor permanent magnet synchronous machine for hybrid electric vehicle," *IEEE Trans. Transport. Electrific.*, vol. 5, no. 4, pp. 1383–1394, Dec. 2019.

[9] S.-C. Carpiuc, "Rotor temperature detection in permanent magnet synchronous machine-based automotive electric traction drives," *IEEE Trans. Power Electron.*, vol. 32, no. 3, pp. 2090–2097, Mar. 2017.

[10] J. Wu, J. Wang, C. Gan, Q. Sun, and W. Kong, "Efficiency optimization of PMSM drives using field-circuit coupled FEM for EV/HEV applications," *IEEE Access*, vol. 6, pp. 15192–15201, 2018.

[11] B. Mashadi and S. A. M. Emadi, "Dual-mode power-split transmission for hybrid electric vehicles," *IEEE Trans. Veh. Technol.*, vol. 59, no. 7, pp. 3223–3232, Sep. 2010.

[12] P. Zheng, J. Bai, C. Tong, Y. Sui, Z. Song, and Q. Zhao, "Investigation of a novel radial magnetic-field-modulated brushless double-rotor machine used for HEVs," *IEEE Trans. Magn.*, vol. 49, no. 3, pp. 1231–1241, Mar. 2013.

[13] C. M. Martinez, X. Hu, D. Cao, E. Velenis, B. Gao, and M. Wellers, "Energy management in plug-in hybrid electric vehicles: Recent progress and a connected vehicles perspective," *IEEE Trans. Veh. Technol.*, vol. 66, no. 6, pp. 4534–4549, Jun. 2017.

[14] H. Wang, Y. Huang, A. Khajepour, and Q. Song, "Model predictive control-based energy management strategy for a series hybrid electric tracked vehicle," *Appl. Energy*, vol. 182, pp. 105–114, Nov. 2016.

[15] K.-C. Kim, "A novel calculation method on the current information of vector inverter for interior permanent magnet synchronous motor for electric vehicle," *IEEE Trans. Magn.*, vol. 50, no. 2, pp. 829–832, Feb. 2014.

[16] K. T. Chau and C. C. Chan, "Emerging energy-efficient technologies for hybrid electric vehicles," *Proc. IEEE*, vol. 95, no. 4, pp. 821–835, Apr. 2007.

[17] P. Zheng, Z. Song, J. Bai, C. Tong, and B. Yu, "Research on an axial Magnetic-Field-Modulated brushless double rotor machine," *Energies*, vol. 6, no. 9, pp. 4799–4829, Sep. 2013.

[18] J. Bai, P. Zheng, C. Tong, Z. Song, and Q. Zhao, "Characteristic analysis and verification of the magnetic-field-modulated brushless double-rotor machine," *IEEE Trans. Ind. Electron.*, vol. 62, no. 7, pp. 4023–4033, Jul. 2015.

[19] Z. Xiang, L. Quan, X. Zhu, and L. Wang, "A brushless double mechanical port permanent magnet motor for plug-in HEVs," *IEEE Trans. Magn.*, vol. 51, no. 11, pp. 1–4, Nov. 2015.
[20] L. Z. Xu, R. Li, and W. T. Song, "Permanent magnetic toroidal drive with half stator," *Adv. Mech. Eng.*, vol. 9, no. 1, pp. 1–7, Jan. 2017.
[21] X. Liu and H. D. Wang, "Analytical calculation and analysis of air gap magnetic field for electromechanical integrated toroidal drive," *Adv. Mech. Eng.*, vol. 11, no. 12, pp. 1–13, Dec. 2019.

XIN LIU received the B.S. and Ph.D. degrees in mechanical engineering from Yanshan University, Hebei, China, in 2004 and 2009, respectively. From 2018 to 2019, she was a Visiting Scholar with the Department of Mechanical Engineering, Virginia Polytechnic Institute and State University, Blacksburg, Virginia, USA. She is currently an Associate Professor with Tiangong University. Her main research interests include electrical machines and drives, drive motor system for hybrid electric vehicles, electromechanical drive systems, and control strategy.

HAO FENG was born in Datong, Shanxi, China, in 1996. He is currently pursuing the master's degree with Tianjin Polytechnic University. His main research interest includes toroidal stator motor for hybrid electric vehicle.

XIAOYUAN WANG was born in Hebei, China, in 1962. He received the B.E. and M.E. degrees in electrical engineering from Tianjin University, Tianjin, China, in 1982 and 1985, respectively, and the Ph.D. degree in electrical engineering from the Shenyang University of Technology, Shenyang, China, in 2006. Since 2007, he has been a Professor with the School of Electrical and Information Engineering, Tianjin University. His current research interests include the design of electrical machines, drive motor system for electric vehicles, motors for high speed applications, and the research of axial flux permanent magnet machines.